Reliability Engineering and System Safety 229 (2023) 108848

Contents lists available at ScienceDirect

Reliability Engineering and System Safety

journal homepage: www.elsevier.com/locate/ress

Modeling dynamic environment effects on dependent failure processes with varying failure thresholds

Bei Wu, Xiaohua Wei, Yamei Zhang, Sijun Bai *

Northwestern Polytechnical University, School of Management, Xi'an, 710072, China

ARTICLE INFO

Keywords:
Markovian environment
Degradation modeling
Random shock
Reliability index
Real-time maintenance
Periodical inspection

ABSTRACT

Devices usually fail due to multiple dependent competing failure processes resulting from internal degradation and random shocks, whose behavior may vary in different environments. This paper focuses on systems suffering from randomly occurring shocks described by Poisson processes and internal degradation characterized by linear path models simultaneously, where the wear rate, shock arrival rate, shock load size, and shock damage amount are modulated by Markovian environments, especially the hard failure threshold differs in distinct environments. Reliability analysis is performed where analytical formulas and simulation algorithms for computing reliability indexes of systems are provided, such as the reliability function. Two maintenance models are developed for systems, including a real-time maintenance policy where the computation formula for the availability function is derived, and a periodic inspection policy in which an optimization model is proposed to find the optimal inspection interval that minimizes the average long-run cost rate. Finally, an illustrative example of floating offshore wind turbine systems is given to demonstrate possible applications of the developed models and proposed methods.

1. Introduction

In this article, we investigate the effect of the dynamic environment on a single-component system that experiences multiple dependent competing failure processes (MDCFPs) resulting from a linear degradation process and randomly occurring shocks. Two correlated failure processes are considered including soft and hard failures. A hard failure arises out of the stress from the shock arrival process, where the shock arrival rate, shock load size, and shock damage amount are modulated by Markovian environments, especially the failure threshold. A soft failure occurs when the total amount of the system degradation hits a preset threshold, caused conjointly by the gradual degradation and additional abrupt damages due to random shocks.

Since many products usually experience dynamic environments during their lifetimes, such as seasonal changes and mode switches, a considerable number of researchers have used stochastic process models to characterize dynamically evolving environments. For example, Markov switching models are commonly used to describe the dynamic environment in the field of system performance, finance and so on, which assume that the environment evolution of the system is governed by a finite-state Markov process [1–3]. Particularly, Markov processes are applied in the reliability field to analyze the stochastic processes in a repairable system [4]. For example, Xiang et al. [5] develop a condition-based maintenance policy for a system, which operates in an environment that is modeled by a continuous-time Markov chain with three states. Shen and Cui [6] consider a multi-state repairable system subject to continuous degradation whose regimes are driven by dynamically evolving environments. Shen et al. [7] present a model for systems subject to several imperfect maintenance actions before each replacement, in which the degradation behavior of the system varies in different environments. Hu et al. [8] propose a condition-based maintenance model which considered imperfect maintenance and replacement for multi-state systems that operate under different environmental conditions, whose evolution is governed by a Markov process. These studies focus on the degradation process of the system, however, ignore the influence of random shocks.

Systems inevitably undergo random shocks during operation, which not only accelerate the degradation process of the system but also lead to hard failures. Note that some studies have attempted to construct models to describe systems exposed to random shocks, and these models can be divided into five categories: (1) extreme shock models, where a system fails when the magnitude of the shock is greater than a predetermined threshold [9,10]; (2) cumulative shock models, where a system fails when the accumulative shock damage reaches a fixed threshold [11–13]; (3) δ-shock models, where a system fails when the interval time between two consecutive shocks is shorter than a fixed

* Corresponding author.
E-mail address: baisj@nwpu.edu.cn (S. Bai).

https://doi.org/10.1016/j.ress.2022.108848
Received 20 April 2022; Received in revised form 16 September 2022; Accepted 18 September 2022
Available online 22 September 2022

Nomenclature

χ	soft failure threshold
ξ_i	hard failure threshold under environment i
$Z(t)$	Markov process that describes the evolution of the environment over time
$\boldsymbol{S}$	finite state space of $Z(t)$
$\boldsymbol{\alpha}$	initial distribution vector of $Z(t)$
$\boldsymbol{Q}$	infinitesimal generator matrix of $Z(t)$
$\boldsymbol{\pi(t)}$	transition probability matrix of $Z(t)$
$W(t)$	cumulative natural wear up to time t
$\mathbb{R}+$	set of all positive real numbers
r_i	linearly wear rate when $Z(t)=i(i\in\boldsymbol{S})$
λ_i	shock arrivals rate when $Z(t)=i(i\in\boldsymbol{S})$
$N_i(t)$	number of shocks occurred in time interval $(0,t]$ under environment i
$L_{i,j}$	load magnitude of the jth shock under environment i
$Y_{i,j}$	damage amount caused by the jth shock under environment i
$\vartheta(t)$	total damage amount caused by random shocks up to time t
$X(t)$	overall degradation amount up to time t
$M_{i,j}$	hard failure margin
$\mathbb{M}_{[0,t]}$	historical minimum margin from the beginning up to time t
$\Theta(t)$	probability that the system does not experience hard failure until time t
$P_i\{\cdot\}$	conditional probability that environment i starts running at time $t=0$
$\boldsymbol{e_i}$	row vector with ith element 1 and remaining elements 0
$\mathbf{1}$	column vector with entries being one
T_k	kth system lifetime under the real-time maintenance policy
M_k kth	repair time under the real-time maintenance policy
τ	inspection interval length
$\hat{T}_k$	kth system lifetime under the periodic inspection policy
$\hat{R}_k$	kth renewal cycle length under the periodic inspection policy
$A(t)(A_i(t))$	unconditional (conditional) availability function
$R(\chi,t)(R_i(\chi,t))$	unconditional (conditional) reliability function
$F(\chi,t)(F_i(\chi,t))$	unconditional (conditional) cumulative distribution function of system lifetime
$\mathbb{E}[\cdot](\mathbb{E}_i[\cdot])$	unconditional (conditional) expectation
C_d	penalty cost per unit time due to downtime
C_i	cost of a single inspection
C_r	cost of a single replacement
$C(t)$	total cumulative cost until time t

Acronym

MDCFP	multiple dependent competing failure process
FOWT	floating offshore wind turbine
HPP	homogeneous Poisson process
i.i.d.	independent and identically distributed
CDF	cumulative distribution function
PDF	probability density function
LST	Laplace–Stieltjes transform
LT	Laplace transform
MCS-SL	Monte-Carlo simulation algorithms for computing system lifetime

threshold δ [14,15]; (4) run shock models, where a system fails due to a sequence of shocks exceeding a critical size [16]; (5) mixed shock models [17,18]. In the present paper, we assume that random shocks affect systems in two different ways: on the one hand, they can destroy systems due to additional degradation amount; on the other hand, they can cause hard failure once the magnitude of the shock reaches the hard failure threshold.

Based on the fact that most systems in practical engineering undergo shocks and internal degradation jointly during their service life, several researchers have made efforts to develop models for systems that simultaneously experience these two failure processes since Lemoine and Wenocur [19] started their research on this issue. There are two streams of research that try to identify how multiple failure processes of the system cause the system to fail. Some studies seek to illustrate that these processes are regarded as independent of each other, for example, see Deloux et al. [20], Liu et al. [21], Wang et al. [22]; while others generally believe that they are dependent structures, called MDCFPs, which can be mainly categorized into two directions. On the one hand, some rest on the assumption that internal degradation depends on random shocks, which suppose that shocks can affect the degradation process in four ways: (1) accelerate degradation by causing a sudden jump in the amount of degradation [23,24]; (2) result in higher degradation rates [25]; (3) decline the level of degradation threshold [26,27]; (4) influence on the failure rate of the system [28]. On the other hand, conversely, some consider that random shocks depend on degradation, where assume that the degradation process can affect shocks by leading to a higher arrival intensity [29] or increasing the probability of fatal shocks [30]. However, these works do not incorporate the effect of dynamic environments, especially the varying failure threshold due to the environment evolution.

Studies for systems with varying failure thresholds have attracted lots of scholars in recent years, which mainly focus on two aspects. The first one is related to soft failure thresholds. For example, Wang et al. [31] propose the use of a threshold zone denoted by a distribution rather than a single threshold line. Chehade et al. [32] present a convex quadratic formulation to online estimate the failure threshold distribution of an operating unit. Gao et al. [33] develop a multi-phase degradation model to describe the sudden changes in failure thresholds and parameters. Li et al. [34] design an optimal warranty policy for deteriorating products, where truncated distributions are used to model the random failure threshold. The second one is devoted to hard failure thresholds. For instance, Rafiee et al. [35] derive a condition-based maintenance model for varying hard failure thresholds due to changes in degradation. Hao and Yang [36] develop a new reliability model to describe the effect of harmful shocks on temporal degradation performance, degradation rates and hard failure threshold levels. Chang et al. [37] extend the previous models by incorporating the effects of the degradation levels on both the degradation rates and the hard failure thresholds. However, the environment evolution of the system is neglected in the above-mentioned papers.

The hard failure of the system arises out of sudden shocks. In engineering practice, dynamic environments may significantly influence the ability of the system to resist damage from shocks, resulting in the hard failure threshold of the system changes with the environment over time. For example, floating offshore wind turbines (FOWTs) are vulnerable

to the natural environment with prominent seasonal characteristics, typically including typhoons, waves, water depths, sea fog, etc, which is reflected in the following aspect: The tension of mooring lines is subject to wind speed or water depths, whose status is affected by seasonal changes. An increase in wind speed or water depths implies a higher breakage risk of mooring lines, which indicates that hard failure thresholds vary with the environment. Neglecting the environmental characteristics of the hard failure threshold may lead to additional maintenance and incur unnecessary high costs. Meanwhile, the degradation behavior of FOWTs is significantly affected by the environment because different temperature and humidity conditions will lead to distinct aging rates. Therefore, in this paper, we focus on the variation in hard failure processes as well as soft failure processes of the system which is affected by dynamic environments.

The scientific contribution of the present article to the existing literature on reliability modeling and engineering practice is as follows.

- A system subject to both linear degradation and random shocks in dynamic environments is investigated, whose wear rate, shock arrival rate, shock load size, and shock damage amount are affected by environments, especially the hard failure threshold varies with the environment.
- Reliability analysis is performed on systems experiencing MDCFPs in dynamic environments, where explicit formulas and Monte-Carlo simulation algorithms for computing system lifetime (MCS-SL) are provided.
- Two maintenance policies are designed for systems, including the real-time maintenance policy in which the analytical expression of the availability function is derived, and the periodic inspection policy in which the optimal inspection interval is obtained.
- An illustrative example of the FOWT system is presented to demonstrate possible applications of models and methods.

The remainder of this paper is organized as follows. Section 2 develops a reliability model for systems subject to MDCFPs in dynamic environments with varying failure thresholds, which gives basic assumptions, analytical formulas, and simulation algorithms for computing reliability functions. Section 3 proposes a real-time maintenance policy and derives the explicit formula for computing the availability function. A periodical inspection policy is presented in Section 4, where an optimization model is developed to find the optimal inspection interval. A case study of the FOWT system is provided in Section 5 to illustrate the obtained methods and formulas. Finally, conclusions are given in Section 6.

2. Reliability analysis of MDCFPs under dynamic environments

In this section, a reliability model for systems that experience both linear degradation and random shock processes simultaneously in dynamic environments will be derived. With respect to constructing a specific but realistic model, the following assumptions are made.

2.1. Modeling of systems subject to MDCFPs under dynamic environments

(2.1.1) The system simultaneously experiences internal degradation and random shocks during its lifetime, whose behaviors are affected by the operating environment. Assume that the system is placed into service at time $t = 0$ and operates in K different environments. The random evolution of environments are governed by an irreducible continuous-time Markov process $\{Z(t), t \geq 0\}$ on finite state space $\boldsymbol{S} = \{1, 2, \ldots, K\}$ with initial distribution vector $\boldsymbol{\alpha} = \{\alpha_i, i \in \boldsymbol{S}\}$, infinitesimal generator matrix $\boldsymbol{Q} = \{q_{ij}, i, j \in \boldsymbol{S}\}$ and transition probability matrix $\boldsymbol{\pi}(t) = \{\pi_{ij}(t), i, j \in \boldsymbol{S}\}$.

(2.1.2) Over time, the system undergoes a continuous natural wear process, whose behavior within different environments can be characterized by different linear degradation path models. In general, the cumulative degradation amount caused by internal degradation at time t is denoted by $\{W(t), t \geq 0\}$. Define a positive function $r : \boldsymbol{S} \to \mathbb{R}^+$ such that whenever $Z(t) = i$, the system wears linearly at a rate r_i $(r_i > 0, i \in \boldsymbol{S})$, where $\mathbb{R}^+$ represents the set of all positive real numbers. Note that the system starts operating from time $t = 0$, then the cumulative natural wear of the system at time t can be expressed as $W(t) = W(0) + \int_0^t r_{Z(u)} du$. By convention, it is assumed that $W(0) = 0$, i.e. the system is put into service at time $t = 0$ without any prior aging, and then $W(t)$ is well defined for each $t \geq 0$ [38].

(2.1.3) At the same time, the system is exposed to shocks which have an impact on the natural degradation process, which is reflected in that shocks can accelerate degradation by causing a sudden jump in the amount of degradation. Shocks occur randomly in time and are affected by the dynamic environment in the following aspects:
(1) the shock arrival rate: Arrivals of random shocks under environment i are governed by a homogeneous Poisson process (HPP) $N_i(t)$ with rate λ_i, where $N_i(t)$ denotes the number of shocks occurred in time interval $(0, t]$ under environment i.
(2) the load magnitude: The load magnitude of the jth shock under environment i is denoted by $L_{i,j}$, and $\{L_{i,j}\}_{j=1}^{\infty}$ are independent and identically distributed (i.i.d.) random variables with cumulative distribution function (CDF) $F_{L_i}(l) = P\{L_i \leq l\}$ and probability density function (PDF) $f_{L_i}(l)$.
(3) the hard failure threshold: When a shock comes to the system under environment i with magnitude not less than the hard failure threshold ξ_i, the system will fail immediately, i.e, a hard failure occurs.
(4) the damage amount: The damage amount caused by the jth shock under environment i is denoted by $Y_{i,j}$, and $\{Y_{i,j}\}_{j=1}^{\infty}$ are i.i.d. random variables with CDF $F_{Y_i}(l) = P\{Y_i \leq l\}$ and PDF $f_{Y_i}(l)$.

(2.1.4) Under the framework of MDCFPs, the system fails when the total damage amount caused by degradation and random shocks up to time t exceeds the threshold level χ, i.e, a soft failure occurs. The cumulative damage amount caused by random shocks up to time t within environment i is denoted by $\{\vartheta_i(t), t \geq 0\}$, which can be expressed as

$$\vartheta_i(t) = \begin{cases} \sum_{j=1}^{N_i(t)} Y_{ij}, & if \quad N_i(t) \geq 1, \\ 0, & if \quad N_i(t) = 0. \end{cases}$$

Herein, the total damage amount caused by random shocks up to time t can be expressed as $\vartheta(t) = \vartheta(h) + \vartheta_i(t-h)$, where $Z(h^-) \neq i$ and for $\forall s \in [h, t]$, $Z(s) = i$. Then the overall degradation amount of the system accumulated up to time t can be expressed as

$$X(t) \triangleq W(t) + \vartheta(t).$$

By convention, it is assumed $X(0) = 0$.

2.2. Analytical methods for calculating reliability functions

In terms of Section 2.1, the system reliability at time t refers to the probability that not only the total damage amount caused by degradation and random shocks accumulated up to time t does not exceed the soft failure threshold, but also the load size of each shock that occurred before time t is not greater than the corresponding hard failure threshold. In other words, the system reliability is the probability that neither a soft failure nor a hard failure occurs until time t.

In order to calculate reliability functions, it is necessary to analyze the hard failure process of the considered system firstly. To this end,

a concept of hard failure margin $M_{i,j}$ is introduced to characterize the difference between the load magnitude of each shock $L_{i,j}$ and the corresponding hard failure threshold ξ_i. Herein, the historical minimum margin from the beginning up to time t is denoted by $\mathbb{M}_{[0,t]}$, and then the probability that the system does not experience hard failure can be expressed as

$$\Theta(t) \triangleq P\{\mathbb{M}_{[0,t]} > 0\}.$$

Then, the system reliability can be given as

$$\begin{aligned} R(\chi,t) &\triangleq P\{X(t) \le \chi, \mathbb{M}_{[0,t]} > 0\} \\ &= \boldsymbol{\alpha} P\{X(t) \le \chi, \mathbb{M}_{[0,t]} > 0 | Z(0) = i\} \\ &= \boldsymbol{\alpha} P\{X(t) \le \chi, \mathbb{M}_{[0,t]} > 0, Z(t) = j | Z(0) = i\}\mathbf{1} \\ &\triangleq \boldsymbol{\alpha} \boldsymbol{R}_{ij}(\chi,t)\mathbf{1}, \end{aligned} \tag{1}$$

where $\mathbf{1}$ refers to a column vector of K ones, and $R_{ij}(\chi,t)$ is the ijth element of a $K\times K$ probability matrix $\boldsymbol{R}(\chi,t)$. By convention, let $P_i\{\cdot\} = P\{\cdot \mid Z(0) = i\}$ denote the conditional probability that environment i starts running at time $t = 0$.

Let $\varepsilon(\varepsilon > 0)$ denote a tiny time increment, and let δ_{ij} be an indicator function that takes value 1 when $i = j$ and value 0 when $i \ne j$. Due to the fact that $Z(t)$ is a continuous-time homogeneous Markov process, which is independent of the shock arrival process and the degradation process, we have

$$\begin{aligned} &R_{ij}(\chi, t+\varepsilon) \\ &= \sum_{k\in \boldsymbol{S}} P\left\{X(t+\varepsilon) \le \chi, \mathbb{M}_{[0,t+\varepsilon]} > 0, Z(t+\varepsilon) = j, \right. \\ &\quad \left. Z(t) = k \mid Z(0) = i\right\} \\ &= \sum_{k\in \boldsymbol{S}} P\left\{X(t+\varepsilon) \le \chi, \mathbb{M}_{[0,t+\varepsilon]} > 0, Z(t+\varepsilon) = j \mid Z(t) = k, \right. \\ &\quad \left. Z(0) = i\right\} \times P\{Z(t) = k \mid Z(0) = i\} \\ &= \sum_{k\in \boldsymbol{S}} P\left\{X(t+\varepsilon) \le \chi, \mathbb{M}_{[0,t+\varepsilon]} > 0, Z(t+\varepsilon) = j \mid Z(t) = k\right\} \\ &\quad \times P\{Z(t) = k \mid Z(0) = i\} \\ &= \sum_{k\in \boldsymbol{S}} \pi_{kj}(\varepsilon) P\left\{X(t+\varepsilon) \le \chi, \mathbb{M}_{[0,t+\varepsilon]} > 0, Z(t) = k \mid Z(0) = i\right\}. \end{aligned} \tag{2}$$

For the HPP $N_k(t)$, it is well-known that

$$\begin{cases} P\{N_k(t+\varepsilon) - N_k(t) = 0 \mid Z(t) = k\} = 1 - \lambda_k\varepsilon + o(\varepsilon), \\ P\{N_k(t+\varepsilon) - N_k(t) = 1 \mid Z(t) = k\} = \lambda_k\varepsilon + o(\varepsilon), \\ P\{N_k(t+\varepsilon) - N_k(t) \ge 2 \mid Z(t) = k\} = o(\varepsilon). \end{cases}$$

Then, conditioning on the number of shocks during time interval $(t, t+\varepsilon)$ and the damage amount caused by shocks, Eq. (2) can be written as

$$\begin{aligned} &R_{ij}(\chi, t+\varepsilon) \\ &= \sum_{k\in \boldsymbol{S}} \pi_{kj}(\varepsilon) \sum_{n=0}^{\infty} P\left\{X(t+\varepsilon) \le \chi, \mathbb{M}_{[0,t+\varepsilon]} > 0, \right. \\ &\quad Z(t) = k \mid N_k(t+\varepsilon) - N_k(t) = n, Z(0) = i\Big\} \\ &\qquad \times P\{N_k(t+\varepsilon) - N_k(t) = n \mid Z(0) = i\} \\ &= \sum_{k\in \boldsymbol{S}} \pi_{kj}(\varepsilon)[(1-\lambda_k\varepsilon) P\left\{X(t+\varepsilon) \le \chi, \mathbb{M}_{[0,t+\varepsilon]} > 0, \right. \\ &\quad Z(t) = k \mid N_k(t+\varepsilon) - N_k(t) = 0, Z(0) = i\Big\} \\ &\qquad + \lambda_k\varepsilon P\left\{X(t+\varepsilon) \le \chi, \mathbb{M}_{[0,t+\varepsilon]} > 0, \right. \\ &\quad \left. Z(t) = k \mid N_k(t+\varepsilon) - N_k(t) = 1, Z(0) = i\right\} + o(\varepsilon)] \\ &= \sum_{k\in \boldsymbol{S}} \pi_{kj}(\varepsilon)[(1-\lambda_k\varepsilon) P\left\{X(t) \le \chi - r_k\varepsilon, \mathbb{M}_{[0,t]} > 0, Z(t) = k \mid Z(0) = i\right\} \\ &\qquad + \lambda_k\varepsilon \int_0^{\chi} P\left\{X(t) \le \chi - r_k\varepsilon - y_k, \mathbb{M}_{[0,t+\varepsilon]} > 0, \right. \\ &\quad \left. Z(t) = k \mid Z(0) = i\right\} F_{L_k}(\xi_k) F_{Y_k}(\mathrm{dy}) + o(\varepsilon)] \\ &= \sum_{k\in \boldsymbol{S}} \pi_{kj}(\varepsilon)[(1-\lambda_k\varepsilon) R_{ik}(\chi - r_k\varepsilon, t) \\ &\quad + \lambda_k\varepsilon \int_0^{\chi} R_{ik}(\chi - r_k\varepsilon - y_k, t) F_{L_k}(\xi_k) F_{Y_k}(\mathrm{dy}) + o(\varepsilon)]. \end{aligned} \tag{3}$$

By replacing $\pi_{ij}(t)$ into the Eq. (3), we have

$$\begin{aligned} R_{ij}(\chi, t+\varepsilon) =& (1-\lambda_j\varepsilon) R_{ij}(\chi - r_j\varepsilon, t) + \varepsilon \sum_{k\in \boldsymbol{S}} (1-\lambda_k\varepsilon) R_{ik}(\chi - r_k\varepsilon, t) q_{kj} \\ &+ \varepsilon\lambda_j F_{L_j}(\xi_j) \int_0^{\chi} R_{ij}(\chi - r_j\varepsilon - y_j, t) F_{Y_j}(\mathrm{dy}) \\ &+ \varepsilon^2 \sum_{k\in \boldsymbol{S}} \lambda_k q_{kj} \int_0^{\chi} R_{ik}(\chi - r_k\varepsilon - y_k, t) F_{Y_k}(\mathrm{dy}) + o(\varepsilon). \end{aligned} \tag{4}$$

Dividing both sides of Eq. (4) by the time increment ε ($\varepsilon \to 0$) yields a simplified partial differential equation with the expression as

$$\begin{aligned} &\frac{\partial R_{ij}(\chi,t)}{\partial t} + \frac{\partial R_{ij}(\chi,t)}{\partial \chi} r_j \\ &= -\lambda_j R_{ij}(\chi,t) + \sum_{k\in \boldsymbol{S}} R_{ik}(\chi,t) q_{kj} + \lambda_j F_{L_j}(\xi_j) \int_0^{\chi} R_{ij}(\chi - y_j, t) F_{Y_j}(\mathrm{dy}), \end{aligned}$$

which can be written in matrix form as

$$\frac{\partial \boldsymbol{R}(\chi,t)}{\partial t} + \frac{\partial \boldsymbol{R}(\chi,t)}{\partial \chi}\boldsymbol{r} = -\boldsymbol{R}(\chi,t)\lambda + \boldsymbol{R}(\chi,t)\boldsymbol{Q} + [\boldsymbol{R}(\cdot,t) * \boldsymbol{Y}(\cdot)](\chi)\lambda\boldsymbol{L}, \tag{5}$$

where $\boldsymbol{r} \triangleq \mathrm{diag}\{r_1, r_2, \dots, r_K\}$, $\lambda \triangleq \mathrm{diag}\{\lambda_1, \lambda_2, \dots, \lambda_K\}$, $\boldsymbol{L} \triangleq \mathrm{diag}\{F_{L_1}(\xi_1), F_{L_2}(\xi_2), \dots, F_{L_K}(\xi_K)\}$, $\boldsymbol{Y}(y) \triangleq \mathrm{diag}\{F_{Y_1}(y), F_{Y_2}(y), \dots, F_{Y_K}(y)\}$ representing the Markov-modulated wear rates matrix, the shock arrival rate matrix, the shock load magnitude matrix, and the shock-induced damage matrix respectively, and $[\boldsymbol{R}(\cdot,t) * \boldsymbol{Y}(\cdot)](\chi)$ refers to each entry of $\boldsymbol{R}(\chi,t)$ convolved with $\boldsymbol{Y}(y)$.

By taking the Laplace–Stieltjes transform (LST) to both sides of Eq. (5) with respect to χ, we can obtain a first-order, ordinary differential equation regarding t as

$$\frac{\partial \tilde{\boldsymbol{R}}(u,t)}{\partial t} + u\tilde{\boldsymbol{R}}(u,t)\boldsymbol{r} = -\tilde{\boldsymbol{R}}(u,t)\lambda + \tilde{\boldsymbol{R}}(u,t)\boldsymbol{Q} + \tilde{\boldsymbol{R}}(u,t)\tilde{\boldsymbol{Y}}(u)\lambda\boldsymbol{L}, \tag{6}$$

where u is a complex number; $\tilde{\boldsymbol{R}}(u,t)$ is the matrix LST of $\boldsymbol{R}(\chi,t)$ with respect to χ, whose ijth entry is given by

$$\tilde{R}_{ij}(u,t) = \int_0^{\infty} e^{-u\chi} R_{ij}(\mathrm{d}\chi, t).$$

Based on Eq. (6), we may write

$$\frac{\partial \tilde{\boldsymbol{R}}(u,t)}{\partial t} + \tilde{\boldsymbol{R}}(u,t)[u\boldsymbol{r} + \lambda - \boldsymbol{Q} - \tilde{\boldsymbol{Y}}(u)\lambda\boldsymbol{L}] = \boldsymbol{0}. \tag{7}$$

Combined with $\tilde{\boldsymbol{R}}(u,0) = \boldsymbol{I}$, we have

$$\tilde{\boldsymbol{R}}(u,t) = \exp\{[\boldsymbol{Q} + \tilde{\boldsymbol{Y}}(u)\lambda\boldsymbol{L} - u\boldsymbol{r} - \lambda]t\}.$$

Then, according to Eq. (1), the LST of the unconditional reliability function of the system regarding χ can be given by

$$\tilde{R}(u,t) = \boldsymbol{\alpha}\exp\{[\boldsymbol{Q} + \tilde{\boldsymbol{Y}}(u)\lambda\boldsymbol{L} - u\boldsymbol{r} - \lambda]t\}\mathbf{1}.$$

And furthermore, the Laplace transform (LT) of the unconditional reliability function of the system regarding χ can be given by

$$R^*(u,t) = \frac{\tilde{R}(u,t)}{u} = \frac{\boldsymbol{\alpha}\exp\{[\boldsymbol{Q} + \tilde{\boldsymbol{Y}}(u)\lambda\boldsymbol{L} - u\boldsymbol{r} - \lambda]t\}\mathbf{1}}{u}, \tag{8}$$

where $R^*(u,t)$ is the LST of $R(\chi,t)$ with respect to χ, whose ijth entry is given by

$$R^*_{ij}(u,t) = \int_0^{\infty} e^{-ut} R_{ij}(\chi,t)dt.$$

Therefore, by taking inverse Laplace transforms of $R^*(u,t)$ with respect to u, the system reliability $R_{ij}(\chi,t)$ can be obtained.

For a fixed soft failure threshold χ, let T_k $(k = 1, 2, \dots)$ denote the kth system lifetime, and T_1 refers to the first system lifetime whose CDF is given by $F(\chi,t) = P\{T_1 \le t\}$. Let $F(\chi,t)$ and $F_i(\chi,t)$ represent the unconditional and conditional CDFs of T_1. Then, according to the dual

relationship between it and the reliability function, the LST of $F(\chi,t)$ regarding χ can be obtained as

$$\tilde{\bar{F}}(u,t) = 1 - \boldsymbol{\alpha}\exp\{[\boldsymbol{Q} + \tilde{\boldsymbol{Y}}(u)\lambda\boldsymbol{L} - u\boldsymbol{r} - \lambda]t\}\mathbf{1}, \tag{9}$$

and

$$\tilde{\bar{F}}_i(u,t) = 1 - \boldsymbol{e}_i\exp\{[\boldsymbol{Q} + \tilde{\boldsymbol{Y}}(u)\lambda\boldsymbol{L} - u\boldsymbol{r} - \lambda]t\}\mathbf{1}, \tag{10}$$

where $\boldsymbol{e}_i$ is row vector with ith element 1 and remaining elements 0.

In addition, denote the moment of the nth power of the system lifetime as $\phi^n(\chi) = \mathbb{E}[T_1^n]$, and in order to get its computation formula, define the LST of $\tilde{F}(u,t)$ with respect to t as $\hat{\tilde{F}}(u,s) = \int_0^\infty e^{-st}\tilde{F}(u,\mathrm{d}t)$, and then the LST of $\phi^n(\chi)$ with respect to χ is given by

$$\begin{aligned}\tilde{\phi}^n(u) &= (-1)^n \frac{\partial \hat{\tilde{F}}(u,s)}{\partial s^n}\bigg|_{s=0} \\ &= n!\boldsymbol{\alpha}[u\boldsymbol{r} + \lambda - \tilde{\boldsymbol{Y}}(u)\lambda\boldsymbol{L} - \boldsymbol{Q}]^{-n}\mathbf{1}.\end{aligned} \tag{11}$$

Similarly, the LST of the conditional of the nth system lifetime can be expressed by

$$\begin{aligned}\tilde{\phi}_i^n(u) &= (-1)^n \frac{\partial \hat{\tilde{F}}_i(u,s)}{\partial s^n}\bigg|_{s=0} \\ &= n!\boldsymbol{e}_i[u\boldsymbol{r} + \lambda - \tilde{\boldsymbol{Y}}(u)\lambda\boldsymbol{L} - \boldsymbol{Q}]^{-n}\mathbf{1}.\end{aligned} \tag{12}$$

Of note, the LST of the expectation of the system lifetime $\mathbb{E}[T_1]$ regarding χ is given by

$$\tilde{\phi}^1(u) = \boldsymbol{\alpha}[u\boldsymbol{r} + \lambda - \tilde{\boldsymbol{Y}}(u)\lambda\boldsymbol{L} - \boldsymbol{Q}]^{-1}\mathbf{1}. \tag{13}$$

2.3. Simulation methods for calculating reliability functions

This section is devoted to providing a simulation method for calculating the reliability function of the system subject to MDCFPs under Markovian environments, which can be applied to verify the correctness of the derived analytical formulas. The simulated value of the reliability function can be obtained by the following steps:

- Generate N system lifetimes by exploiting the MCS-SL algorithm, denoted as $T_{1,j}(j = 1,\ldots,N)$.
- For each generated time t, Kaplan–Meier (K–M) method is applied to predict the reliability function [39], i.e,

$$R(t) = \frac{\sum_{j=1}^{N} I_{\{t\le T_{1,j}\}}}{N}, \text{ for } t > 0.$$

MCS-SL Algorithm: MCS procedure of computing system lifetime

1 Initialize χ, N_d, $\boldsymbol{Q}$, $\boldsymbol{\pi}$, $k(k \in \boldsymbol{S})$, λ_k, r_k, ξ_k, μ_{Y_k}, δ_{Y_k}, μ_{L_k}, δ_{L_k}.
2 Default aw, t, t_1, t_2, t_3 and j are 0.
3 Generate a random number u_1 following the exponential distribution with parameter $-q_{kk}$, let $\Delta t = u_1/N_d$, and set $t_1 \leftarrow t_1 + u_1$.
4 Generate a random number u_2 following the exponential distribution with parameter λ_k, and set $t_2 \leftarrow t_2 + u_2$.
5 Generate random numbers ss and sl following normal distributions with parameters $N(\mu_{Y_k}, \delta_{Y_k}^2)$ and $N(\mu_{L_k}, \delta_{L_k}^2)$ respectively.
6 If $t_3 + j * \Delta t < t_2 < t_3 + (j+1) * \Delta t$, go to Step 7; otherwise, go to Step 9.
7 If $sl < \xi_k$, then go to Step 8; otherwise, $t \leftarrow t_2$, go to Step 12.
8 If $aw + r_k * \Delta t + ss < \chi$, then $aw \leftarrow aw + r_k * \Delta t + ss$, $j \leftarrow j+1$, and go to Step 4; otherwise, $t \leftarrow t_2$, go to Step 12.
9 If $aw + r_k * \Delta t < \chi$, then $aw \leftarrow aw + r_k * \Delta t$, $j \leftarrow j+1$, and go to Step 10; otherwise, $t \leftarrow t_3 + (j+1) * \Delta t$, go to Step 12.
10 If $j < N_d$, then go to Step 6; otherwise, go to Step 11.
11 Generate a random number u_3, find v satisfying $\sum_{l=1}^{l=v-1}\pi_{kl} < u_3 < \sum_{l=1}^{l=v}\pi_{kl}$, set $k \leftarrow v$, $t_3 \leftarrow t_1$, $t_2 \leftarrow t_1$, and go to Step 3.
12 At this time, t refers to the first passage time. End.

Note that in the MCS-SL algorithm, the load size of shocks is assumed to be normal distributions with distinct parameters μ_{L_k} and δ_{L_k} for different environments, while the damage size of shocks is also assumed to be normal distributions with distinct parameters μ_{Y_k} and δ_{Y_k} for different environments.

3. Real-time maintenance policy

In this section, an inspection policy with real-time maintenance is considered for systems subject to MDCFPs under Markovian environments, which is conducive to timely detection of system failures and reduction of loss costs.

3.1. Modeling assumptions for real-time maintenance policy

The following detailed assumptions are made to underpin the real-time maintenance policy which is considered in this article.

(3.1.1) Once the system fails whether it is hard or soft, it can be checked in time and then a real-time maintenance action will be implemented immediately, which means that there is zero time lag between system failures and maintenance. The maintenance is supposed to be perfect which can repair the system to the as-good-as-new condition.

(3.1.2) All processes such as the natural wear, the environment state evolution and the shock arrival are suspended during each repair. This indicates that the switching process of the environment state only occurs while the system is operating, and the state evolution of the environment will restart once the maintenance action is completed.

Let $\{t_k^-\}_{k=1}^\infty$ and $\{t_k^+\}_{k=1}^\infty$ respectively indicate the start and end time instants during the kth system repair time under the real-time maintenance policy. By convention, $t_0^+ = 0$ is the start time of the new system. Further, $M_k = t_k^+ - t_k^- \left(k \in N^+\right)$ is defined as the time spent during repair after the kth failure with PDF $f_M(x)$. Let $T_k = t_k^- - t_{k-1}^+ \left(k \in N^+\right)$ represent the kth system lifetime, and $\{T_k\}_{k=1}^\infty$ are i.i.d. random variables with CDF $F(\chi,t) = P\{T_1 \le t\}$. Repair times are assumed to be independent of system lifetimes. Based on the above assumptions, Fig. 1 shows a possible sample path realization with real-time maintenance for systems subject to MDCFPs under Markovian environments.

3.2. Analytical method for deriving the system availability

According to the assumption that the environment evolution of the system will restart at $\{t_k^+\}_{k=0}^\infty$, $\{Z(t_k^+), t_k^+\}_{k=0}^\infty$ forms a homogeneous Markov renewal process whose semi-Markov kernel is defined by $\boldsymbol{V}(t) = \left[V_{ij}(t), i,j \in \boldsymbol{S}\right]$ with

$$\begin{aligned}V_{ij}(t) &= P\{Z(t_1^+) = j, t_1^+ - t_0^+ \le t \mid Z(t_0^+) = i\} \\ &= P\{Z(M_1 + T_1) = j, M_1 + T_1 \le t \mid Z(0) = i\}.\end{aligned} \tag{14}$$

Taking the LST of both sides of Eq. (14), we have

$$\begin{aligned}\tilde{V}_{ij}(s) &= \mathbb{E}_i[e^{-s(T_1+M_1)}\cdot\delta_{\{Z(M_1+T_1)=j\}}]\\ &= \int_0^{+\infty}\mathbb{E}_i[e^{-s(T_1+M_1)}\cdot\delta_{\{Z(M_1+T_1)=j\}}\mid M_1=t]d\varphi(t)\\ &= \int_0^{+\infty}e^{-st}\mathbb{E}_i[e^{-s(T_1)}\cdot\delta_{\{Z(T_1)=j\}}]d\varphi(t)\\ &= \int_0^{+\infty}e^{-st}\int_0^{+\infty}\mathbb{E}_i[e^{-s(T_1)}\\ &\quad\cdot\delta_{\{Z(T_1)=j\}}\mid T_1=\psi]dP\{T_1\le\psi\mid Z(0)=i\}d\varphi(t)\\ &= \int_0^{+\infty}e^{-st}\int_0^{+\infty}e^{-s\psi}\mathbb{E}_i[\delta_{\{Z(\psi)=j\}}]F_i(\chi,d\psi)d\varphi(t)\\ &= \int_0^{+\infty}\int_0^{+\infty}e^{-s(t+\psi)}\mathbb{E}_i[\delta_{\{Z(\psi)=j\}}]F_i(\chi,d\psi)d\varphi(t).\end{aligned}\tag{15}$$

Based on Eq. (15), it is necessary to obtain $\mathbb{E}_i[\delta_{\{Z(\psi)=j\}}]$. Now, we are going to define a $K\times K$ matrix $\boldsymbol{Y}(\psi)$ whose ijth entry is given by $Y_{ij}(\psi)=\mathbb{E}_i[\delta_{\{Z(\psi)=j\}}]$, and then, Eq. (15) can be rewritten as

$$\tilde{V}_{ij}(s)=\int_0^{+\infty}\int_0^{+\infty}e^{-s(t+\psi)}Y_{ij}(\psi)F_i(\chi,d\psi)d\varphi(t).\tag{16}$$

For $i\neq j$, we have

$$\begin{aligned}Y_{ij}(\psi) &= P\{Z(\psi)=j\mid Z(0)=i\}\\ &= \sum_{k\in\boldsymbol{S},k\neq i}P\left\{Z(\psi)=j,Z(\theta_1)=k,\theta_1>\psi\mid Z(0)=i\right\}\\ &\quad+\sum_{k\in\boldsymbol{S},k\neq i}P\left\{Z(\psi)=j,Z(\theta_1)=k,\theta_1\leqslant\psi\mid Z(0)=i\right\}\\ &= \sum_{k\in\boldsymbol{S},k\neq i}\int_0^{\psi}P\left\{Z(\psi)=j\mid Z(\theta_1)=k,\theta_1=v,\right.\\ &\quad\left.Z(0)=i\right\}dP\{Z(\theta_1)=k,\theta_1\leqslant v\mid Z(0)=i\}\\ &= \sum_{k\in\boldsymbol{S},k\neq i}\int_0^{\psi}P\{Z(\psi-v)=j\mid Z(0)=k\}dP\{Z(\theta_1)=k,\\ &\quad\theta_1\leqslant v\mid Z(0)=i\}\\ &= \sum_{k\in\boldsymbol{S},k\neq i}\int_0^{\psi}e^{q_{ii}v}q_{ik}Y_{kj}(\psi-v)dv,\end{aligned}\tag{17}$$

where θ_k is defined as the moment of the kth environment change, and for $i=j$,

$$\begin{aligned}Y_{ii}(\psi) &= P\{Z(\psi)=i\mid Z(0)=i\}\\ &= P\left\{Z(\psi)=i,\theta_1>\psi\mid Z(0)=i\right\}\\ &\quad+P\left\{Z(\psi)=i,\theta_1\leqslant\psi\mid Z(0)=i\right\}\\ &= e^{q_{ii}\psi}+\sum_{k\in\boldsymbol{S},k\neq i}\int_0^{\psi}P\left\{Z(\psi)=i\mid Z(\theta_1)=k,\theta_1=v,\right.\\ &\quad\left.Z(0)=i\right\}dP\{Z(\theta_1)=k,\theta_1\leqslant v\mid Z(0)=i\}\\ &= e^{q_{ii}\psi}+\sum_{k\in\boldsymbol{S},k\neq i}\int_0^{\psi}P\{Z(\psi-v)=i\mid Z(0)=k\}dP\{Z(\theta_1)=k,\\ &\quad\theta_1\leqslant v\mid Z(0)=i\}\\ &= e^{q_{ii}\psi}+\sum_{k\in\boldsymbol{S},k\neq i}\int_0^{\psi}e^{q_{ii}v}q_{ik}Y_{ki}(\psi-v)dv.\end{aligned}\tag{18}$$

Taking LTs of both sides of Eqs. (17) and (18) yields, for $i\neq j$,

$$Y_{ij}^*(s)=\sum_{k\in\boldsymbol{S},k\neq i}\frac{q_{ik}}{s-q_{ii}}Y_{kj}^*(s),\tag{19}$$

and for $i=j$,

$$Y_{ii}^*(s)=\frac{1}{s-q_{ii}}+\sum_{k\in\boldsymbol{S},k\neq i}\frac{q_{ik}}{s-q_{ii}}Y_{ki}^*(s).\tag{20}$$

To express Eqs. (19) and (20) in matrix form, we further define three matrices which are

$$\tilde{\boldsymbol{V}}(s)=[\tilde{V}_{ij}(s),i,j\in\boldsymbol{S}],$$

$$\boldsymbol{D}^*(s)=\mathrm{diag}\left\{\frac{1}{s-q_{11}},\cdots,\frac{1}{s-q_{KK}}\right\},$$

$$\boldsymbol{Q}_1=\begin{pmatrix}0 & q_{12} & \cdots & q_{1(K-1)} & q_{1K}\\ q_{21} & 0 & \cdots & q_{2(K-1)} & q_{2K}\\ \vdots & \vdots & \ddots & \vdots & \vdots\\ q_{(K-1)1} & q_{(K-1)2} & \cdots & 0 & q_{(K-1)K}\\ q_{K1} & q_{K2} & \cdots & q_{K(K-1)} & 0\end{pmatrix},$$

and then, we have

$$\boldsymbol{Y}^*(s)=\boldsymbol{D}^*(s)+\boldsymbol{D}^*(s)\boldsymbol{Q}_1\boldsymbol{Y}^*(s),\tag{21}$$

which follows that

$$\boldsymbol{Y}^*(s)=[\boldsymbol{I}-\boldsymbol{D}^*(s)\boldsymbol{Q}_1]^{-1}\boldsymbol{D}^*(s).\tag{22}$$

To obtain the system availability, we now introduce a fresh stochastic process $\{U(t):t\geq 0\}$ which is defined as

$$U(t)=\begin{cases}1, & \text{the system is working at time } t,\\ 0, & \text{the system is failed at time } t.\end{cases}\tag{23}$$

Define the conditional system availability as $A_i(t)$, which satisfies

$$\begin{aligned}A_i(t) &\triangleq P\{U(t)=1\mid Z(0)=i\}\\ &= P\left\{U(t)=1,t<T_1\mid Z(0)=i\right\}\\ &\quad+P\left\{U(t)=1,T_1\le t<T_1+M_1\mid Z(0)=i\right\}\\ &\quad+P\left\{U(t)=1,T_1+M_1\le t\mid Z(0)=i\right\}\\ &= R_i(\chi,t)\\ &\quad+\sum_{j\in\boldsymbol{S}}\int_0^t P\{U(t)=1\mid Z(t_1^+)=j,t_1^+=u\}dP\{Z(t_1^+)=j,\\ &\quad t_1^+\le u\mid Z(0)=i\}\\ &= R_i(\chi,t)+\sum_{j\in\boldsymbol{S}}\int_0^t A_j(t-u)dV_{ij}(u).\end{aligned}\tag{24}$$

Taking the LT of both sides of Eq. (24) regarding t yields,

$$A_i^*(s)=R_i^*(\chi,s)+\sum_{j\in\boldsymbol{S}}\tilde{V}_{ij}(s)A_j^*(s),\tag{25}$$

which follows that

$$\boldsymbol{A}^*(s)=\boldsymbol{R}^*(\chi,s)\,\boldsymbol{1}+\tilde{\boldsymbol{V}}(s)\boldsymbol{A}^*(s),\tag{26}$$

where $\boldsymbol{A}^*(s)=\left[A_1^*(s),\ldots,A_K^*(s)\right]^T$. Here by, the T stands for transpose, which means to change rows into columns. Combined with the initial distribution $\boldsymbol{\alpha}$, the LT of the system availability is given by

$$A^*(s)=\boldsymbol{\alpha}[\boldsymbol{I}-\tilde{\boldsymbol{V}}(s)]^{-1}\boldsymbol{R}^*(\chi,s)\,\boldsymbol{1}.\tag{27}$$

Therefore, by taking inverse Laplace transforms of $A^*(s)$ with respect to s based on Eq. (27), the system availability $A(t)$ can be obtained with numerical methods.

4. Periodic inspection policy

In this section, an inspection policy with periodic check intervals is considered for systems subject to MDCFPs under Markovian environments, where the status of the system is unknown unless an inspection action is carried out.

4.1. Modeling assumptions for periodic inspection policy

The following detailed assumptions are made to underpin the periodic inspection policy which is considered in this article.

(4.1.1) As a system is placed into service, the current status can be identified only by inspection which is carried out periodically every τ ($\tau>0$), and a corrective replacement is implemented instantaneously with a new and identical one once the system

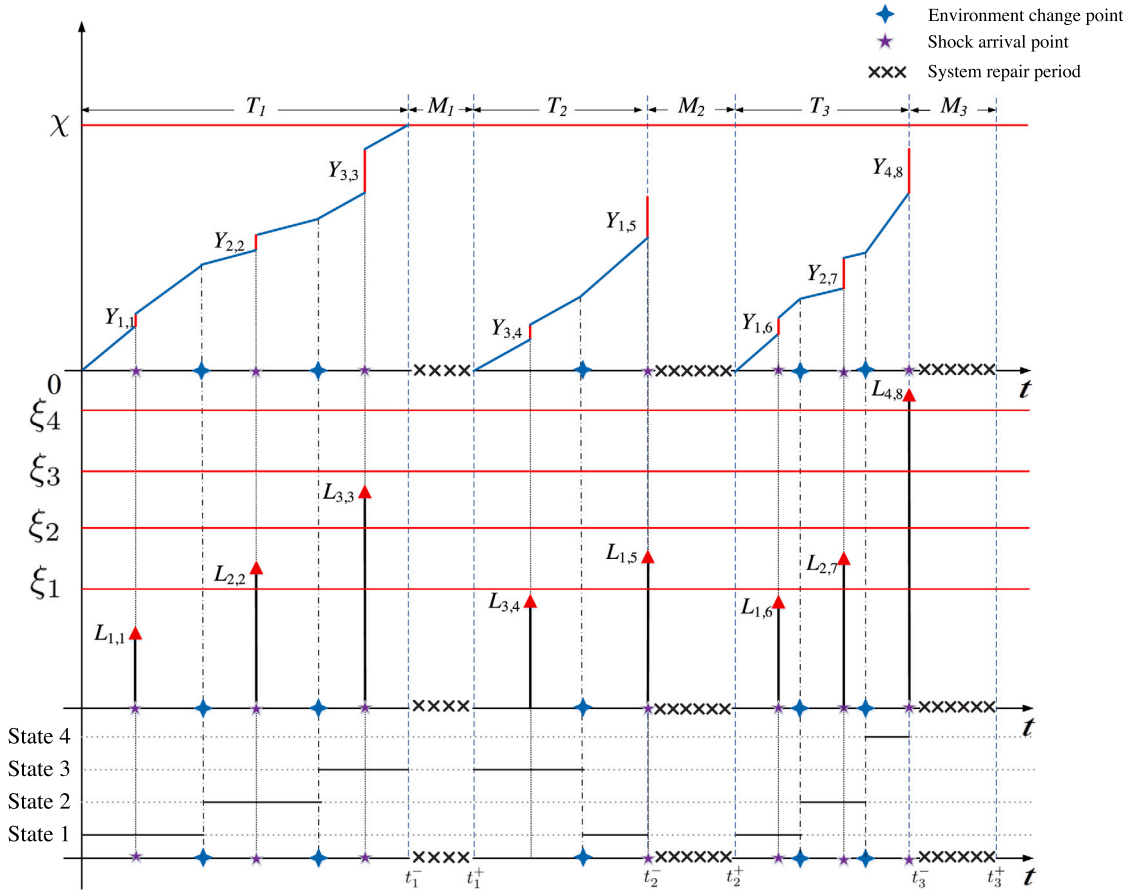

Fig. 1. A possible sample path realization with the real-time maintenance for systems subject to MDCFPs under Markovian environments.

is detected as a failure. The inspection is supposed to be perfect, non-destructive, and instantaneous.

(4.1.2) The system is out of work during downtime, i.e. the natural wear process, the environment state evolution process, and the shock arrival process are all suspended accordingly. Once the maintenance action is completed, the system resumes operation, meanwhile, the environment state evolution process of the system restarts immediately.

On the one hand, Assumption 4.1.1 indicates that the hidden failures of the system cannot be discovered until the next scheduled inspection. On the other hand, in common with the model assumption in Wu et al. [40], Assumption 4.1.2 describes the restriction on the evolution process of the environment state, which is in accordance with engineering practice. For distinguish between Section 3, let $\{\hat{t}_k^-\}_{k=1}^{\infty}$ and $\{\hat{t}_k^+\}_{k=1}^{\infty}$ represent the kth failure time and the kth renewal time of systems respectively under the periodic inspection policy, where the interval between two consecutive corrective replacements can be regarded as a renewal cycle. Further, $\hat{R}_k = \hat{t}_k^+ - \hat{t}_{k-1}^+ \left(k \in N^+\right)$ is defined as the kth renewal time length of systems. Let $\hat{T}_k = \hat{t}_k^- - \hat{t}_{k-1}^+ \left(k \in N^+\right)$ represent the kth system lifetime, and $\{\hat{T}_k\}_{k=1}^{\infty}$ are i.i.d. random variables with CDF $F(\chi,t) = P\{\hat{T}_1 \le t\}$. In order to illustrate the above assumptions, a possible sample path realization with the periodic inspection for systems subject to MDCFPs under Markovian environments is shown in Fig. 2.

4.2. Analytical method for deriving the optimal inspection interval

In this section, $\hat{R}_1$ refers to the first renewal time length of the system. Then in terms of Assumption 4.1.1, the corrective replacement must be carried out at inspection points, which indicates that $\hat{R}_1$ explicitly depends on $\hat{T}_1$ according to $\hat{R}_1 = \inf\left\{t \in Y : t > \hat{T}_1\right\}$, where $Y = \{k\tau : k \in \mathbb{N}^+\}$ is defined as the set of inspection time points.

Then, let $\tilde{r}$ represent the minimum natural wear rate with expression as $\tilde{r} \triangleq \min\left\{r_1, r_2, \ldots, r_K\right\}$, and according to Kharoufeh et al. [38], the random variable $\hat{T}_1$, namely the first system lifetime, is bounded above by $\chi/\tilde{r}$, so it can be obtained that $F_i(\chi,t) = 1$ when $t \ge \chi/\tilde{r}$. As for the expected length of the renewal cycle $\mathbb{E}[\hat{R}_1]$, by conditioning on $\hat{T}_1$, we have

$$\mathbb{E}[\hat{R}_1] = \mathbb{E}\left[\mathbb{E}_i[\hat{R}_1]\right] = \sum_{i\in S}\alpha_i\mathbb{E}_i[\hat{R}_1] = \sum_{i\in S}\alpha_i\int_0^{\infty}\mathbb{E}_i\left[\hat{R}_1 \mid \hat{T}_1 = t\right]F_i(\chi,\mathrm{d}t),$$

where

$$\mathbb{E}_i[\hat{R}_1 \mid \hat{T}_1 = t] = \begin{cases} \tau, & 0 \le t < \tau, \\ 2\tau, & \tau \le t < 2\tau, \\ \vdots & \\ n\tau, & (n-1)\tau \le t < n\tau, \\ \vdots & \end{cases}$$

which follows that

$$\mathbb{E}[\hat{R}_1] = \sum_{i\in S}\alpha_i\left\{\sigma\tau - \tau\sum_{n=0}^{\sigma-1}F_i(\chi,n\tau)\right\}, \tag{28}$$

where $\sigma = \min\{n \ge 1 : n\tau \ge \chi/\tilde{r}\}$. The detailed proof of Eq. (28) refers to Wu and Cui [41].

It is common for practical engineering that decision-makers always need to balance the downtime loss due to equipment failures with inspection costs and maintenance costs. By minimizing the expected cost [42,43], we can obtain the optimal policy of maintenance decision. To this end, a cost-based optimal model that incorporates reliability and preventive maintenance for periodic inspection policy we develop

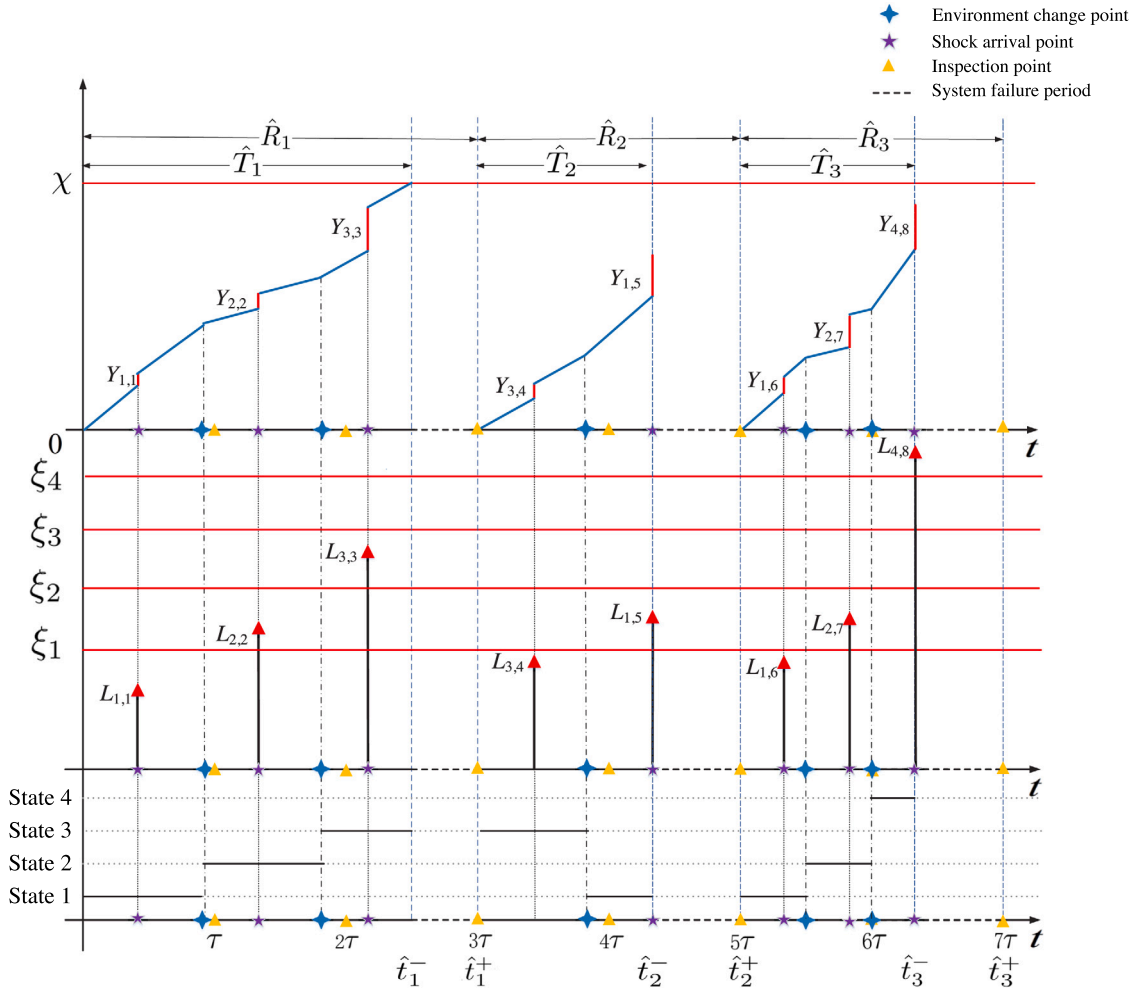

Fig. 2. A possible sample path realization with the periodic inspection for systems subject to MDCFPs under Markovian environments.

in order to benefit practitioners from optimizing the system over the long run and obtaining minimal average long-run costs.

Let C_d, C_i, and C_r represent the penalty cost per unit time due to downtime, the cost of a single inspection, and the cost of a single replacement respectively. Meanwhile, let $C(t)$ denote the total cumulative cost until time t. According to the basic renewal theory, minimizing the average cost rate of a preventive maintenance policy could minimize the average long-run cost [44,45]. Herein, the average long-run cost rate is given by

$$\lim_{t\to\infty}\frac{C(t)}{t}=\frac{\mathbb{E}[C]}{\mathbb{E}[\hat{R}_1]}, \tag{29}$$

where $\mathbb{E}[C]$ denotes the expected total cost in a renewal cycle, and $\mathbb{E}[\hat{R}_1]$ denotes the expected length of the renewal cycle.

Therefore, it is necessary to obtain $\mathbb{E}[C]$, which can be divided into three parts, i.e.,

$$\mathbb{E}[C]=C_d\mathbb{E}[D_c]+C_i\mathbb{E}\left[M_c\right]+C_r,$$

where $\mathbb{E}[D_c]$ denotes the expected system downtime within a renewal cycle, and $\mathbb{E}\left[M_c\right]$ refers to the expected number of inspections within a renewal cycle. Concerning the expected system downtime within a renewal cycle, based on Eq. (28), we have

$$\begin{aligned}\mathbb{E}[D_c]&=\mathbb{E}[\hat{R}_1]-\mathbb{E}\left[\hat{T}_1\right]\\&=\sum_{i\in S}\alpha_i\left\{\sigma\tau-\tau\sum_{n=0}^{\sigma-1}F_i(\chi,n\tau)\right\}-\mathbb{E}\left[\hat{T}_1\right],\end{aligned} \tag{30}$$

where $\mathbb{E}\left[\hat{T}_1\right]$ can be obtained by taking the inverse LST on $\tilde{\phi}^1(u)$ with respect to χ for a given soft failure threshold. As for the expected number of inspections within a renewal cycle, it can be expressed as

$$\begin{aligned}\mathbb{E}[M_c]&=\sum_{i\in S}\alpha_i\mathbb{E}_i[M_c]\\&=\sum_{i\in S}\alpha_i\sum_{n=1}^{\infty}nP_i\left\{\hat{R}_1=n\tau\right\}\\&=\sum_{i\in S}\alpha_i\sum_{n=1}^{\infty}n\int_0^{\infty}P_i\left\{\hat{R}_1=n\tau\mid\hat{T}_1=t\right\}F_i(\chi,\,\mathrm{d}t)\\&=\sum_{i\in S}\alpha_i\sum_{n=1}^{\sigma}n\Delta_i(\chi,n\tau),\end{aligned} \tag{31}$$

where $\Delta_i(\chi,n\tau)\triangleq F_i(\chi,n\tau)-F_i(\chi,(n-1)\tau)$.

It is often encountered in engineering practice that the inspection interval τ is set to be not less than a certain fixed duration, say ρ, or a multiple of ρ [41]. Hence, an optimization model is developed which takes the minimal average long-run cost rate as the objective, and the inspection interval τ as the decision variable. The optimal inspection interval τ^* satisfies

$$\begin{cases}\min_{\tau}\ \dfrac{\sum_{i\in S}\sum_{n=1}^{\sigma}n\alpha_i\Delta_i(\chi,n\tau)C_i+\sum_{i\in S}\tau\sigma\alpha_iC_d-\sum_{i\in S}\sum_{n=0}^{\sigma-1}\tau\alpha_iF_i(\chi,n\tau)C_d-\mathbb{E}[\hat{T}_1]C_d+C_r}{\sum_{i\in S}\tau\sigma\alpha_i-\sum_{i\in S}\sum_{n=0}^{\sigma-1}\tau\alpha_iF_i(\chi,n\tau)}\\ \text{s.t. }\tau=k\rho,\quad k\in\mathbb{N}^+\end{cases}$$

where $\mathbb{N}^+$ represents the set of all positive integers.

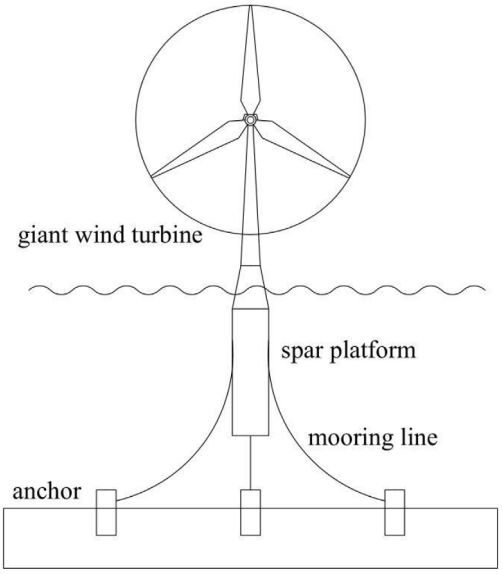

Fig. 3. Structure diagram of the Hywind Demo.

The enumeration method is applied to solving the developed optimization problem. To determine the optimal inspection interval τ^*, we can calculate the long-run average cost rate for various values of τ, and find out τ^* corresponding to the minimum long-run average cost rate. Then, based on the above, the optimal inspection interval τ^* that minimizes the average long-run cost rate can be obtained with numerical methods.

5. A case study of FOWT systems

This section focuses on a case study of FOWT systems that experiences MDCFPs under Markovian environments, in order to illustrate the proposed models and methods.

5.1. Background

Recently, offshore wind power production has become a key element of a more sustainable future energy. The Hywind Demo, a FOWT developed by Statoil [46], consists of a spar platform that supports a giant wind turbine and a mooring system that attaches the spar structure to the seabed through three separate mooring lines connected to anchors. The structure diagram of the Hywind Demo is shown in Fig. 3.

In practical engineering, the FOWT system usually undergoes two competing failure processes. On the one hand, the FOWT system experiences soft failure processes due to material damage and degeneration. For example, spar foundations are concrete shell structures that are floated onto the seabed, which mainly suffer from corrosion and abrasive wear. On the other hand, the FOWT system is also subject to hard failure processes due to harsh environmental conditions, such as strong wind, monster waves, violent storms, and other abnormal working conditions [47]. For instance, typhoons not only accelerate the material damage and degeneration but also increase the risk of mooring lines breakage [48].

Generally, FOWT systems are working in a dynamic environment, such as operating in different seasons, different water depths or different weather conditions [49]. In this way, on the one hand, the environment has a significant effect on the aging behavior of the concrete shell, because different temperature and humidity conditions lead to distinct aging rates in dynamic environments. On the other hand, behaviors of typhoons vary with distinct environments, reflecting on different frequencies, levels, and damage amount to mooring systems. In addition, seasonal changes can affect sea level, leading to the variation of the tension of mooring lines and thus hard failure thresholds vary.

Therefore, we apply the models and methods developed in this article to investigate FOWT systems that experience two competing failure processes and seasonal changes in the next section.

5.2. Reliability analysis of the study case

FOWT systems are significantly affected by seasonal changes. Swedish and Finnish meteorologists have proposed the concept of thermal criteria, which is made to distinguish between seasons using mean daily temperatures, whose definition is as follows:

- spring, where the mean daily temperature rises from 0 °C to 10 °C for seven consecutive days;
- summer, where the mean daily temperature remains above 10 °C for seven consecutive days;
- autumn, where the mean daily temperature stays below 10 °C for seven consecutive days;
- winter, where the mean daily temperature is consistently below 0 °C for seven consecutive days.

Therefore, it is assumed that a fresh FOWT system is placed into service at time $t = 0$ without any prior degradation, and periodically experiences four different working environments, i.e., spring, summer, autumn and winter, recorded as states 1, 2, 3 and 4 respectively, whose sojourn times are supposed to follow exponential distributions with parameters 6, 3, 6 and 3. That indicates that the average length of spring and autumn is two months, while the average length of summer and winter is four months. Then, the evolution of working environments is governed by a Markov process $Z(t)$, whose infinitesimal generator is

$$\boldsymbol{Q} = \begin{pmatrix} -6 & 6 & 0 & 0 \\ 0 & -3 & 3 & 0 \\ 0 & 0 & -6 & 6 \\ 3 & 0 & 0 & -3 \end{pmatrix}$$

with initial distribution vector $\boldsymbol{\alpha} = (1, 0, 0, 0)$.

Thermal expansion and cold shrinkage are two main influencing factors for cracks in the spar foundation of the FOWT. The temperature difference between the surface and the interior of the concrete shell increases the possibility of cracking. Hence, a linear degradation path model is employed to describe the growth of the crack in the FOWT concrete shell, whose rates in different environment states are assumed to be $r_1 = 0.5$, $r_2 = 1$, $r_3 = 0.7$ and $r_4 = 1.5$, i.e. $\boldsymbol{r} = diag\{0.5, 1, 0.7, 1.5\}$.

Meanwhile, FOWTs are subject to typhoons sometimes, whose occurrence has obvious seasonal characteristics, so assume that the behavior of typhoons in different seasons can be described by different homogeneous Poisson processes, whose arrival rates in different working environments are given as $\lambda_1 = 1$, $\lambda_2 = 6$, $\lambda_3 = 3$ and $\lambda_4 = 1$, i.e. $\lambda = diag\{1, 6, 3, 1\}$.

Typhoons can result in large swings of the spar foundation, which may lead to the acceleration of the system deterioration and the failure of the mooring system. On the one hand, owing to its lower viscosity, the typhoon exerts negative pressure when it waves away from the spar foundation of the FOWT, which accelerates the degradation process of the concrete shell. In different seasons, the damage caused by typhoons on the degradation process of the concrete shell follows the normal distribution with different parameters, i.e. $Y_1 \sim N(1.54, 0.1^2)$, $Y_2 \sim N(1.58, 0.1^2)$, $Y_3 \sim N(1.56, 0.1^2)$, and $Y_4 \sim N(1.52, 0.1^2)$. On the other hand, mooring lines are vital for the station-keeping of FOWTs and the survival of mooring systems, whose tension is significantly affected by typhoons that may make mooring lines prone to fracture failure. Then, the load magnitude of typhoons follows the normal distribution

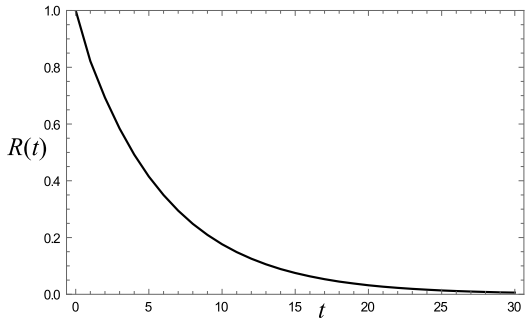

Fig. 4. A plot of reliability function of FOWT system.

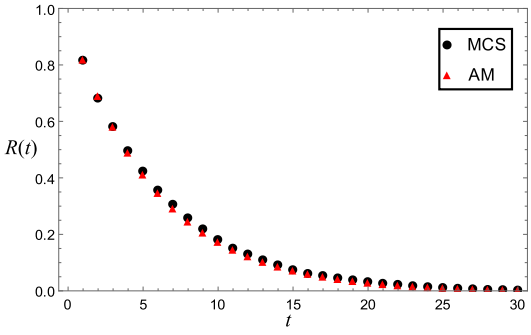

Fig. 5. Curves of reliability functions computed by two methods.

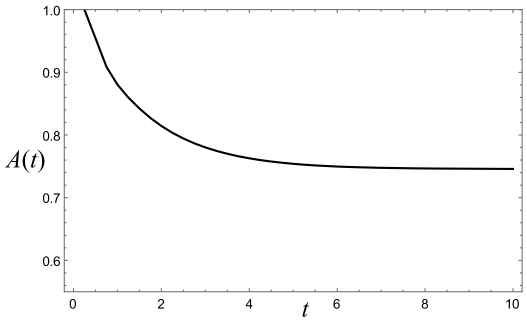

Fig. 6. A plot of availability function of FOWT system.

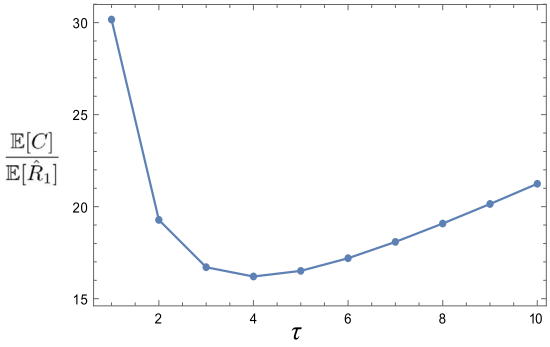

Fig. 7. Average long-run cost rate for FOWT systems.

with different parameters in different environment states, i.e., $L_1 \sim N(0.13, 0.01^2)$, $L_2 \sim N(0.15, 0.01^2)$, $L_3 \sim N(0.14, 0.01^2)$, and $L_4 \sim N(0.11, 0.01^2)$.

The tension of mooring lines is also subject to water depths, whose status is affected by seasonal changes, and a raised water depth can lead to an increase in the possibility of mooring line fracture. To this end, the changing hard failure threshold of the FOWT system refers to the ability to withstand damage from shocks in different environments, which are supposed to be $\xi_1 = 1.74$, $\xi_2 = 1.72$, $\xi_3 = 1.76$, and $\xi_4 = 1.78$. Meanwhile, assume the soft failure threshold $\chi = 500$, indicating that when the crack of the spar foundation reaches 500, the FOWT system loses its function and needs repairing.

According to Section 2.3, the reliability function of the FOWT can be plotted based on the numerical method of the inverse Laplace transform, whose curve is shown in Fig. 4.

It can be observed from Fig. 4 that the reliability function of the FOWT decreases with the increase of time. In order to verify the correctness of the derived formula for the reliability function, the MCS-SL algorithm has been executed to estimate $R(t)$. The curves of reliability functions calculated with the analytical method (AM) and the MCS are plotted in Fig. 5.

As for the real-time maintenance policy, suppose that the repair time $\{M_i\}_{i=1}^{\infty}$ is exponentially distributed with parameter $\eta = 0.5$, and in terms of Eq. (27), the availability function of the FOWT system can be plotted as Fig. 6 shows.

The realization of real-time maintenance depends on the development of sensor technology, and there are restrictions on installation sites and high costs. Therefore, it is necessary to develop a replaceable maintenance strategy to achieve the dual objectives of availability and economy. Suppose that the FOWT system is periodically checked at intervals of duration τ ($\tau > 0$), the cost per unit of downtime is $C_d = 100$, the inspection cost of the FOWT each time is $C_i = 5$, and the replacement cost of the FOWT each time is $C_r = 20$. According to Section 4, the optimal inspection interval τ^* can be obtained by solving the following optimization model:

$$\begin{cases} \min_{\tau} \dfrac{\sum_{i=1}^{4}\sum_{n=1}^{1000} 1.25 n\Delta_i(\chi, n\tau) + 100\left\{\sum_{i=1}^{4}\left[250\tau - 0.25\sum_{i=1}^{4}\sum_{n=1}^{999} F_i(\chi, n\tau)\right] - \mathbb{E}[\hat{T}_1]\right\} + 20}{\sum_{i=1}^{4}\left[250\tau - 0.25\tau\sum_{n=0}^{999} F_i(\chi, n\tau)\right]} \\ \text{s.t. } \tau = k\rho, \quad k \in \mathbb{N}^+ \end{cases}$$

where the minimum feasible inspection interval $\rho = 0.2$. Then, the average long-run cost rate for different values of τ is shown in Fig. 7.

As shown in Fig. 7, the optimal inspection interval to check the FOWT system is $\tau^* = 4$, and the minimization of the average long-run cost rate is 16.207.

5.3. Sensitivity analysis of the study case

In this section, sensitivity analysis is performed to observe the effect of model parameters on the system reliability, availability, and optimal inspection interval. The parameters of interest are the shock arrival rate λ_i, hard failure threshold ξ_i, inspection cost of each time C_i, and replacement cost of each time C_r whose results are provided as follows, by taking model parameters under environment 2 as an example.

By varying the shock arrival rate in environment 2 while fixing other parameters, the results of the system reliability, availability, and average long-run cost rate can be plotted in Fig. 8.

It can be seen from Fig. 8 that, the shock arrival rate can influence the system reliability, availability and optimal inspection interval significantly. When λ_2 is increased progressively from 4 to 8, curves of the system reliability and availability functions both shift to the left, the average long-run cost rate shift to the right, and the optimal inspection interval to check the FOWT system changes from $\tau^* = 5$ to $\tau^* = 3$. It is because a raised λ_i indicates a higher arrival rate of random shocks, which accelerates the failure process of the FOWT system, and increases the total cost.

The results of the reliability, availability and average long-run cost rate can be plotted in Fig. 9 by varying the hard failure threshold in environment 2 while fixing other parameters.

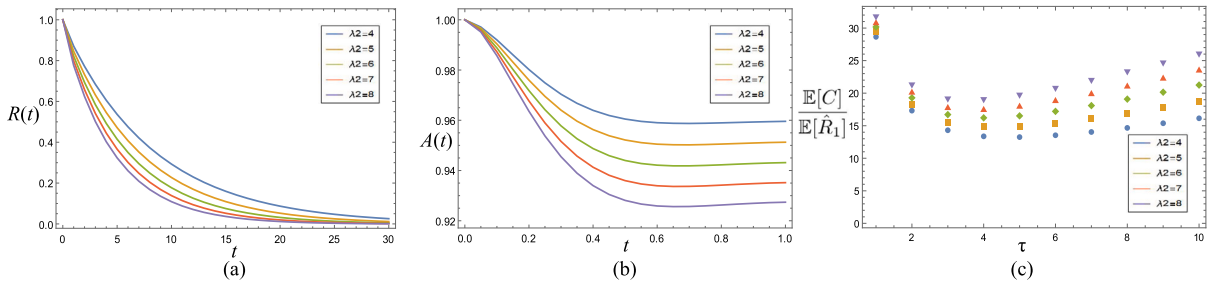

Fig. 8. Sensitivity analysis of reliability, availability and average long-run cost rate on λ_2.

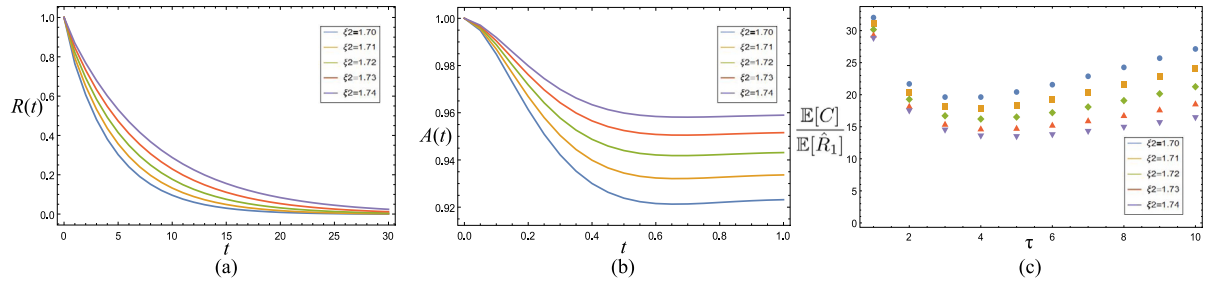

Fig. 9. Sensitivity analysis of reliability, availability and average long-run cost rate on ξ_2.

Fig. 9 shows that the system reliability, availability and optimal inspection interval are sensitive to the hard failure threshold. When ξ_2 is increased progressively from 1.70 to 1.74, both the reliability and availability function shift to the right, the average long-run cost rate shift to the left, and the optimal inspection interval to check the FOWT system changes from $\tau^* = 3$ to $\tau^* = 5$. This is because an increased hard failure threshold implies a better capability to withstand disruptive events, which promotes the performance of the FOWT system and reduces the total cost.

6. Conclusions

In this article, we investigate a system suffering from linear degradation and random shocks, whose wear rate, shock arrival rate, shock load size, and shock damage amount are affected by a dynamic environment, especially hard failure thresholds vary with environments. Reliability analysis is performed on systems subject to MDCFPs including soft failures caused jointly by natural wear and additional abrupt degradation damages due to shocks, and hard failures resulting from the same shock processes. Explicit formulas and simulation algorithms for computing reliability indexes of systems are provided, such as the reliability function. Furthermore, two maintenance policies are presented for systems including a real-time maintenance policy where the computation formula for the availability function is given and a periodical inspection policy in which an optimization model is proposed to find the optimal inspection interval that minimizes the average long-run cost rate. Finally, they are applied to a realistic example considering the FOWT system in order to illustrate the proposed models and obtained results.

Meaningful conclusions can be drawn that an increased shock arrival rate leads to lower system performance, a shorter optimal inspection interval, and a higher cost. Instead, a raised hard failure threshold improves the system performance and prolongs the optimal inspection interval. It is worth noting that this paper is devoted to a single-unit system, which can be further extended to multi-unit systems by considering independent or dependent components. As a preliminary analysis of the maintenance policies for systems, obviously, there are potential other extensions which are worth exploring. In this respect, our paper is limited to the case where the maintenance is supposed to be perfect which can repair the system to the as-good-as-new condition. Therefore, maintenance policies associated with imperfect repair can be considered for a repairable system in future work. Besides that, by relaxing some assumptions made in this paper, further advances can be achieved. For example, more distinct types of shocks may be explored to meet the engineering requirements well. This paper assumed that all shocks can accelerate degradation by causing an abrupt jump in the amount of degradation. With the development of techniques, devices are typically designed to withstand small shock loads. In this case, shocks can be categorized into three shock zones according to their magnitudes: safety zone, damage zone, and fatal zone. Meanwhile, the enumeration method is used to deal with the developed optimal model in this paper, which takes a long time to solve and is prone to fall into the local optimum. Therefore, an effective heuristic algorithm can be introduced for greater operation speed and good performance. In addition, the extension from Markov processes to semi-Markov processes, or from homogeneous Poisson processes to non-homogeneous Poisson processes might be worthing.

CRediT authorship contribution statement

Bei Wu: Conceptualization, Methodology, Software, Formal analysis. **Xiaohua Wei:** Writing – original draft, Writing – review & editing, Software. **Yamei Zhang:** Writing – review & editing, Software. **Sijun Bai:** Writing – review & editing, Supervision.

Declaration of competing interest

The authors declare that they have no known competing financial interests or personal relationships that could have appeared to influence the work reported in this paper.

Data availability

Data will be made available on request.

Acknowledgments

The study is supported by the National Natural Science Foundation of China under grant 72101205 and the Fundamental Research Funds for the Central Universities under grant 3102021XJS05.

References

[1] Hawkes AG, Cui L, Zheng Z. Modeling the evolution of system reliability performance under alternative environments. IIE Trans 2011;43(11):761–72.
[2] Liang X, Wang G, Li H. Pricing credit default swaps with bilateral counterparty risk in a reduced form model with Markov regime switching. Appl Math Comput 2014;230:290–302.
[3] Rotta PN, Valls Pereira PL. Analysis of contagion from the dynamic conditional correlation model with Markov Regime switching. Appl Econ 2016;48(25):2367–82.
[4] Cui L, Li Y, Shen J, Lin C. Reliability for discrete state systems with cyclic missions periods. Appl Math Model 2016;40(23–24):10783–99.
[5] Xiang Y, Cassady CR, Pohl EA. Optimal maintenance policies for systems subject to a Markovian operating environment. Comput Ind Eng 2012;62(1):190–7.
[6] Shen J, Cui L. Reliability performance for dynamic multi-state repairable systems with K regimes. IISE Trans 2017;49(9):911–26.
[7] Shen J, Cui L, Ma Y. Availability and optimal maintenance policy for systems degrading in dynamic environments. European J Oper Res 2019;276(1):133–43.
[8] Hu J, Xu A, Li B, Liao H. Condition-based maintenance planning for multi-state systems under time-varying environmental conditions. Comput Ind Eng 2021;158:107380.
[9] Eryilmaz S, Kan C. Reliability and optimal replacement policy for an extreme shock model with a change point. Reliab Eng Syst Saf 2019;190:106513.
[10] Meango TJ-M, Ouali M-S. Failure interaction model based on extreme shock and Markov processes. Reliab Eng Syst Saf 2020;197:106827.
[11] Montoro-Cazorla D, Pérez-Ocón R. A reliability system under cumulative shocks governed by a BMAP. Appl Math Model 2015;39(23–24):7620–9.
[12] Gong M, Eryilmaz S, Xie M. Reliability assessment of system under a generalized cumulative shock model. Proc Inst Mech Eng 2020;234(1):129–37.
[13] Dong W, Liu S, Bae SJ, Cao Y. Reliability modelling for multi-component systems subject to stochastic deterioration and generalized cumulative shock damages. Reliab Eng Syst Saf 2021;205:107260.
[14] Wang GJ, Peng R. A generalised δ-shock model with two types of shocks. Int J Syst Sci: Oper Logist 2017;4(4):372–83.
[15] Zhao B, Yue D, Liao H, Liu Y, Zhang X. Performance analysis and optimization of a cold standby system subject to δ-shocks and imperfect repairs. Reliab Eng Syst Saf 2021;208:107330.
[16] Ozkut M, Eryilmaz S. Reliability analysis under Marshall–Olkin run shock model. J Comput Appl Math 2019;349:52–9.
[17] Rafiee K, Feng Q, Coit DW. Reliability assessment of competing risks with generalized mixed shock models. Reliab Eng Syst Saf 2017;159:1–11.
[18] Wu B, Cui L, Qiu Q. Two novel critical shock models based on Markov renewal processes. Nav Res Logist 2022;69(1):163–76.
[19] Lemoine AJ, Wenocur ML. On failure modeling. Nav Res Logist Q 1985;32(3):497–508.
[20] Deloux E, Castanier B, Bérenguer C. Predictive maintenance policy for a gradually deteriorating system subject to stress. Reliab Eng Syst Saf 2009;94(2):418–31.
[21] Liu B, Zhang Z, Wen Y, Kang S, Guo Y, Qiu Q. Reliability analysis for complex systems subject to competing failure processes in an uncertain environment. J Intell Fuzzy Systems 2020;39(3):4331–9.
[22] Wang X, Liu B, Zhao X. A performance-based warranty for products subject to competing hard and soft failures. Int J Prod Econ 2021;233:107974.
[23] Che H, Zeng S, Guo J, Wang Y. Reliability modeling for dependent competing failure processes with mutually dependent degradation process and shock process. Reliab Eng Syst Saf 2018;180:168–78.
[24] Yan T, Lei Y, Li N, Wang B, Wang W. Degradation modeling and remaining useful life prediction for dependent competing failure processes. Reliab Eng Syst Saf 2021;212:107638.
[25] Rafiee K, Feng Q, Coit DW. Reliability modeling for dependent competing failure processes with changing degradation rate. IIE Trans 2014;46(5):483–96.
[26] Zhou X, Wu C, Li Y, Xi L. A preventive maintenance model for leased equipment subject to internal degradation and external shock damage. Reliab Eng Syst Saf 2016;154:1–7.
[27] Hao S, Yang J, Ma X, Zhao Y. Reliability modeling for mutually dependent competing failure processes due to degradation and random shocks. Appl Math Model 2017;51:232–49.
[28] Dong W, Liu S, Cao Y, Javed SA. Scheduling optimal replacement policies for a stochastically deteriorating system subject to two types of shocks. ISA Trans 2021;112:292–301.
[29] Liu Y, Wang Y, Fan Z, Bai G, Chen X. Reliability modeling and a statistical inference method of accelerated degradation testing with multiple stresses and dependent competing failure processes. Reliab Eng Syst Saf 2021;213:107648.
[30] Sun F, Li H, Cheng Y, Liao H. Reliability analysis for a system experiencing dependent degradation processes and random shocks based on a nonlinear Wiener process model. Reliab Eng Syst Saf 2021;215:107906.
[31] Wang W, Carr M, Xu W, Kobbacy K. A model for residual life prediction based on Brownian motion with an adaptive drift. Microelectron Reliab 2011;51(2):285–93.
[32] Chehade A, Bonk S, Liu K. Sensory-based failure threshold estimation for remaining useful life prediction. IEEE Trans Reliab 2017;66(3):939–49.
[33] Gao H, Cui L, Kong D. Reliability analysis for a Wiener degradation process model under changing failure thresholds. Reliab Eng Syst Saf 2018;171:1–8.
[34] Li T, He S, Zhao X. Optimal warranty policy design for deteriorating products with random failure threshold. Reliab Eng Syst Saf 2022;218:108142.
[35] Rafiee K, Feng Q, Coit DW. Reliability analysis and condition-based maintenance for failure processes with degradation-dependent hard failure threshold. Qual Reliab Eng Int 2017;33(7):1351–66.
[36] Hao S, Yang J. Reliability analysis for dependent competing failure processes with changing degradation rate and hard failure threshold levels. Comput Ind Eng 2018;118:340–51.
[37] Chang M, Huang X, Coolen FP, Coolen-Maturi T. Reliability analysis for systems based on degradation rates and hard failure thresholds changing with degradation levels. Reliab Eng Syst Saf 2021;216:108007.
[38] Kharoufeh JP, Finkelstein DE, Mixon DG. Availability of periodically inspected systems with Markovian wear and shocks. J Appl Probab 2006;43(2):303–17.
[39] Huang T, Zhao Y, Coit DW, Tang L-C. Reliability assessment and lifetime prediction of degradation processes considering recoverable shock damages. IISE Trans 2021;53(5):614–28.
[40] Wu B, Cui L, Yin J. Reliability and maintenance of systems subject to Gamma degradation and shocks in dynamic environments. Appl Math Model 2021;96:367–81.
[41] Wu B, Cui L. Reliability analysis of periodically inspected systems with competing risks under Markovian environments. Comput Ind Eng 2021;158:107415.
[42] Yang L, Chen Y, Qiu Q, Wang J. Risk control of mission-critical systems:Abort decision-makings integrating health and age conditions. IEEE Trans Ind Inf 2022. http://dx.doi.org/10.1109/TII.2022.3141416.
[43] Qiu Q, Maillart LM, Prokopyev OA, Cui L. Optimal condition-based mission abort decisions. IEEE Trans Reliab 2022. http://dx.doi.org/10.1109/TR.2022.3172377.
[44] Ross SM. Introduction to probability models. Academic Press; 2014.
[45] Gosavi A, Murray SL, Tirumalasetty VM, Shewade S. A budget-sensitive approach to scheduling maintenance in a total productive maintenance (TPM) program. Eng Manag J 2011;23(3):46–56.
[46] Van der Loos A, Normann HE, Hanson J, Hekkert MP. The co-evolution of innovation systems and context: Offshore wind in Norway and the Netherlands. Renew Sustain Energy Rev 2021;138:110513.
[47] Li H, Soares CG, Huang H-Z. Reliability analysis of a floating offshore wind turbine using Bayesian networks. Ocean Eng 2020;217:107827.
[48] Cheng Z, Madsen HA, Chai W, Gao Z, Moan T. A comparison of extreme structural responses and fatigue damage of semi-submersible type floating horizontal and vertical axis wind turbines. Renew Energy 2017;108:207–19.
[49] Lin Z, Liu X, Lotfian S. Impacts of water depth increase on offshore floating wind turbine dynamics. Ocean Eng 2021;224:108697.